Available online at www.sciencedirect.com
SCIENCE DIRECT®
Journal of the European Ceramic Society 25 (2005) 3503–3508
www.elsevier.com/locate/jeurceramsoc

Reaction kinetics in Ti_3SiC_2 synthesis studied by time-resolved neutron diffraction

E. Wu[a,b], D.P. Riley[a], E.H Kisi[a,*], R.I. Smith[c]

[a] *School of Engineering, The University of Newcastle, Callaghan, NSW 2308, Australia*
[b] *Shenyang National Laboratory for Materials Science, Shenyang 110016, PR China*
[c] *ISIS Facility, Rutherford Appleton Laboratory, Chilton, Didcot, Oxon OX11 0QX, UK*

Received 2 June 2004; received in revised form 10 August 2004; accepted 27 August 2004

Abstract

The reactive sintering of 3Ti/SiC/C to form the ternary carbide Ti_3SiC_2, previously found to involve the intermediate phases TiC_x and $Ti_5Si_3C_x$, was investigated by time-resolved neutron powder diffraction. The kinetics of Ti_3SiC_2 formation from the intermediate phases TiC_x, $Ti_5Si_3C_x$ ($x \leq 1$) and a small amount of free C was determined. The crystallization rate of the Ti_3SiC_2 phase was determined through quantitative analyses of the diffraction patterns collected at different temperatures and is initially well-described by the Mehl–Avrami–Johnson equation. The activation energy was found to be 380 ± 10 kJ/mol and the Avrami exponent 3.0 ± 0.2. The Avrami exponent decreases to close to 1 when more than half of the crystallization process was completed. This indicates a change in the mechanism of Ti_3SiC_2 crystal growth from unrestricted two or three-dimensional growth in the *a–b* planes to one-dimensional growth only, due to interaction of the growing disk-like crystals and cessation of growth in the preferred direction.

Keywords: Sintering; Carbides; Kinetics; Ti_3SiC_2; Neutron diffraction

1. Introduction

The last few years have seen strong interest in studies of the ternary carbide Ti_3SiC_2 because of its unique combination of properties.[1–8] Ti_3SiC_2 has been prepared using several different methods.[9–15] Among them the reactive sintering of 3Ti/SiC/C to form Ti_3SiC_2 has been extensively studied since, when coupled with hot pressing, this process can produce fully dense near-single phase Ti_3SiC_2 ceramic.[1,11] To understand the reaction mechanism and its time and temperature dependence, we have studied the process using in situ neutron diffraction techniques.[16,17] By conducting the experiments in situ, the microstructural processes and phase transitions occurring in bulk ceramics are revealed in a time-resolved sequence. The reaction paths revealed by in situ neutron diffraction during the heating of 3Ti/SiC/C mixtures at 10 °C/min and reactive sintering at 1600 °C to synthesise Ti_3SiC_2 were discussed in our previous papers.[16,17] There two well-separated reaction stages were observed. In the first stage the two intermediate phases identified by El-Raghy and Barsoum,[18] TiC_x and $Ti_5Si_3C_x$ ($x \leq 1$), occurred in the sample according to the overall reaction $9Ti + 3SiC + 3C \rightarrow 4TiC_x + Ti_5Si_3C_x + C$ ($x \leq 1$). By 1400 °C all of the Ti has been consumed. In the second stage the two intermediate phases plus a small amount of carbon become the only phases in the system prior to the appearance of the product phase. The intermediate phases react to form Ti_3SiC_2 according to the overall reaction $4TiC_x + Ti_5Si_3C_x + C$ ($x \leq 1$) $\rightarrow 3Ti_3SiC_2$.[17] Based on the concentrations of the Ti_3SiC_2 phase calculated from quantitative phase analysis of the diffraction patterns, formation of Ti_3SiC_2 is slow at temperatures near 1200 °C and, fairly rapid at higher temperatures.[16] However, the kinet-

* Corresponding author. Tel.: +61 2 4921 6213; fax: +61 2 4921 6946.
E-mail address: Erich.Kisi@newcastle.edu.au (E.H Kisi).

0955-2219/$ – see front matter © 2004 Elsevier Ltd. All rights reserved.
doi:10.1016/j.jeurceramsoc.2004.09.005

ics were not quantified in these earlier continuous heating experiments[16,17]—kinetic information is far more readily obtained from isothermal experiments. Knowledge of the reaction kinetics is needed not only for a quantitative description of the temperature-time paths of the reaction, but also for a better understanding of the mechanism of the synthesis process. This paper reports the kinetics of Ti_3SiC_2 formation from the intermediate phases TiC_x, $Ti_5Si_3C_x$ and C in the second sintering stage based upon recent in situ time-resolved neutron diffraction experiments.

2. Experimental procedure and analysis

The experimental procedure is very similar to that used previously.[17] Ti (Aldrich 99.98%), SiC (Performance Ceramics 99.9%) and C (graphite Fluka Chemika 99.9%) powders were mixed in stoichiometric proportions and hand ground under argon. Cylindrical pellets of 16 mm diameter and 15 mm high were cold pressed to (180 MPa) in a hard steel die. Two pellets were stacked vertically to increase the mass of sample within the neutron beam and thereby reduce data collection times. Time-of-flight (TOF) neutron powder diffraction data were collected on the POLARIS[19] medium resolution powder diffractometer at the ISIS pulsed neutron spallation source, Rutherford Appleton Laboratory, UK. A coarse mesh cage made from 0.25 mm diameter Mo wire was used to suspend the samples in the neutron beam inside an evacuated ($\sim 10^{-5}$ Torr) Ta element furnace during the in situ synthesis studies. The furnace was heated up to a predetermined holding temperature at an average rate of 10 °C/min to ensure that the correct mixture of intermediate phases was formed. The samples were then held at temperature for 2.5 h followed by slow cooling to room temperature. The furnace temperature was measured and controlled by two type W5 thermocouples positioned ~1 cm above the sample, in order to limit the amount of extraneous material in the neutron beam. Four heating ramps with holding temperatures of 1450, 1500, 1550 and 1600 °C were employed, respectively, and TOF neutron diffraction patterns were collected as repeated scans of 2.7 min throughout the synthesis process. Provision of collimating slits between the sample and the detector combined with the TOF technique, which enables a complete diffraction pattern to be collected at a single fixed detector position, reduced significantly the intensities and numbers of Bragg reflections arising from the Ta furnace elements and heat shields which appear in the diffraction patterns collected in the $2\theta \sim 90^\circ$ ZnS detector bank.

Structure refinements were conducted by Rietveld analysis using the program GSAS[20] and the refined scale factors were used to conduct quantitative phase analysis (QPA).[21] In the analysis, the refined parameters were: global parameters (diffractometer zero, the coefficients of a polynomial background), parameters refined for all phases (scale factor and lattice parameters) and ones refined only for majority phases (the Gaussian and Lorentzian broadening components of the convoluted TOF profile, thermal parameters, structural variables and x—the site occupancy variable of TiC_x and $Ti_5Si_3C_x$).

Based on the concentrations of the Ti_3SiC_2 phase in the sample calculated from QPA of the TOF diffraction patterns, and assuming that the reaction is described by the Avrami kinetic equation, the kinetics of Ti_3SiC_2 formation expressed as the mol-fraction of the transformed new phase f at any time t can be modeled using the Mehl–Avrami–Johnson (MAJ) equation:[22–25]

$$f(t) = 1 - \exp[-(Kt)^n] \tag{1}$$

here n is the Avrami exponent and K is the reaction rate constant, which is related to the activation energy of the process, E, through an Arrhenius temperature dependence:

$$K(T) = K_0 \exp(-E/RT) \tag{2}$$

where K_0 is the frequency factor, R the gas constant and T the absolute temperature.

Taking the logarithm of Eq. (1) twice:

$$\ln[-\ln(1-f)] = n \ln K + n \ln t \tag{3}$$

A plot of $\ln[-\ln(1-f)]$ versus $\ln t$ for different isotherms will give n and K, and from these the activation energy of the process E can be determined.

Besides those intermediate phases TiC_x and $Ti_5Si_3C_x$ ($x \leq 1$), the growth of Ti_3SiC_2 crystals requires a small amount of free C for the solid state reaction.[16,17] The free C is not crystalline, and can not be determined from quantitative analysis of the diffraction patterns, thus the derived fraction of the transformed Ti_3SiC_2 crystals f could be affected by ignoring this factor. The effect of free C on the calculated fraction f is estimated by adding a stoichiometric amount of free C in the calculation and assuming that the free C is reduced to null while the fraction of the transformed Ti_3SiC_2 crystals f reaches the maximum.

The solid state reaction leading to Ti_3SiC_2 formation requires an incubation time at constant temperature for appreciable reaction products to be observed. It is possible to describe the reaction time as comprised from two components $t = t_i + t_c$, where t_i is incubation time and t_c is the crystallization time. However, t is difficult to measure in our experiments, even though they were conducted isothermally. Due to the large heat capacity of the sample, a considerable period of time is required before the temperature of the sample equilibrated with the furnace temperature, such that in some cases the reaction initiated before sample equilibration at the hold temperature. This incubation time spent at lower temperatures could become quite significant at the higher temperatures when the reaction rate is high.

An iterative method was adopted in our calculation to correct for the effect and access the true incubation time at constant temperature. It can be assumed that the incubation time required for the reaction at low temperature during an exper-

iment would be, in effect, equivalent to a shorter period of time at the hold temperature of the experiment, which can be defined as t_0, so the total reaction time will become $t = t_m + t_0$, where t_m is measured time, and Eq. (1) becomes:

$$f = 1 - \exp[-(K(t_m + t_0))^n] \quad (4)$$

where t_0 is not known, but was defined as 0 for the initial iteration. An initial n and K were derived for each temperature from Eq. (3), and an average activation energy E estimated. Eq. (2) was then used to calculate a new K, which was used in Eq. (4) to calculate a new t_0 for each temperature. Then the new t_0 was used to do the second iteration and so on, until convergence was achieved, in this case, after only three iterations.

3. Results and discussion

An example of the neutron diffraction data and associated Rietveld refinement fit used for quantitative phase analysis is shown in Fig. 1. The agreement between the calculated and the observed data points is very good. The final plots of $\ln[-\ln(1-f)]$ versus $\ln t$ at different temperatures after three iterations are shown in Fig. 2. The value of n for the formation of Ti_3SiC_2 from $4TiC_x + Ti_5Si_3C_x + C$ determined from the measurement of the slopes is 3.0 ± 0.2 and the reaction rate constant K is $1.35 \times 10^{-4}\,s^{-1}$ (1450 °C), $2.84 \times 10^{-4}\,s^{-1}$ (1500 °C), $5.76 \times 10^{-4}\,s^{-1}$ (1550 °C) and $1.13 \times 10^{-3}\,s^{-1}$ (1600 °C), respectively. The activation energy $E = 380 \pm 10$ kJ/mol and $K_0 = 4.45 \times 10^7\,s^{-1}$ in Eq. (2) are derived from the three slopes at 1450, 1500 and 1550 °C in Fig. 2.

In a perfect isothermal experiment at uniform temperature intervals, the lines representing the Arrhenius temperature dependence of the reaction rate constant K on Fig. 2 would be parallel. As seen in Fig. 2, this is most closely observed for the lower portion of the data at 1450 and 1500 °C. As for the plot at 1550 °C, although the correct spacing between the plots is observed, deviations from linearity occur earlier and are larger. For the data at 1600 °C, the deviation is too large and the spacing is not as expected. The plot is much closer to the data for 1550 °C and the raw Arrhenius temperature relation is not valid for data recorded at 1600 °C. The primary reason for this is the incubation time of the reaction. During the lower temperature isothermal holds (1450 and 1500 °C) the reaction rate was relatively low and the bulk of the reaction occurred at the stated temperature. The small fraction of the incubation time that was spent at a lower temperature can therefore be estimated and compensated for according to our corrected timescale. At 1550 °C the fraction of the incubation time occurring before the start of the isothermal hold increased further. However, for the 1600 °C data, the sample actually completed its incubation time while still at lower temperatures and a small amount of Ti_3SiC_2 formed even before the isothermal hold at 1600 °C began. There is potentially an additional effect present in all measurements due to the fact that because the thermocouple was not in contact with the sample, a further lag occurred between the thermocouple indicating the hold temperature and the bulk of the sample reaching this temperature. Hence, the plot for the measurements at 1600 °C actually reflects the reaction at a lower sample temperature. Based on the position of the plot, we can estimate that the sample behaviour during the 1600 °C measurement reflects an actual sample temperature of 1565 °C, some 35 °C lower than the indicated temperature. Assuming this correction to be valid, the K derived from the plot corresponding to 1565 °C is $7.07 \times 10^{-4}\,s^{-1}$. The derived relationship between the fraction of the Ti_3SiC_2 phase and the total reaction time at various temperatures fitted by the MAJ equation is shown in Fig. 3.

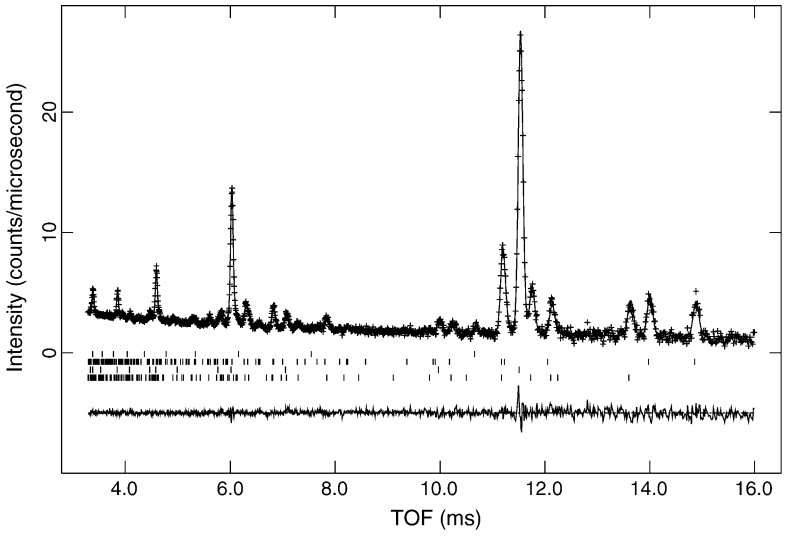

Fig. 1. Rietveld fit to TOF neutron diffraction pattern collected at 1500 °C. Data points are shown as (+) and the calculation as a solid line. The difference profile for the refinement along with reflection markers for the phases Ti_3SiC_2 (bottom), $TiC_{1.0}$ (middle lower), $Ti_5Si_3C_{0.64}$ (middle higher) and reflections from the Ta furnace element (top) are shown below the pattern. TOF (ms) may be converted to d-spacing (Å) by multiplying by 2.19×10^{-4}.

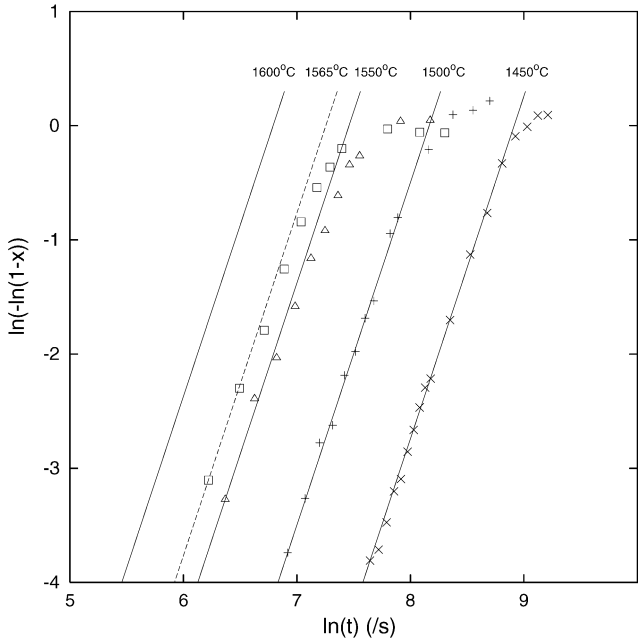

Fig. 2. The function $\ln[-\ln(1-f)]$ vs. $\ln t$ at different temperatures. The straight line at each temperature is drawn according to the fitted values of k_0 and E. The symbol corresponding to each temperature is: (×) 1450 °C, (+) 1500 °C, (△) 1550 °C and (□) 1600 °C.

Recalling that the reaction of TiC_x, $Ti_5Si_3C_x$ and free C to form Ti_3SiC_2 proceeds in the solid state, the reaction kinetics presented here relate to the precipitation and growth of Ti_3SiC_2 crystals. From the plots in Figs. 2 and 3, it can also be noted that the linear Avrami relation between $\ln(-\ln(1-f))$ and $\ln t$ is actually only properly held for the early stages of the crystal growth process, where the Avrami exponent n can be calculated as ∼3. During the later stages of the crystallization, when the fraction of Ti_3SiC_2, f, exceeds ∼0.5 (i.e. $\ln(-\ln(1-f)) \sim -0.37$), the plots start to deviate from the linear relation as shown in Fig. 2, and the Avrami exponent n changes to about 1, and further to about 0, i.e. growth ceases altogether. The Avrami exponent n is a characteristic parameter linked to the morphology of the crystallization process,[26] and a change in the Avrami exponent during the growth of the new phase indicates a change in the mechanism of crystal growth. According to the MAJ theory,[27,28] a value of 3 for the Avrami exponent corresponds to a bulk crystallization process involving either two-dimensional growth with constant nucleation rate, or three-dimensional growth of a constant number of nuclei. In contrast, a value close to 1 corresponds to a predominantly one dimensional crystal growth process. These observations suggest that, after an initial stage of relatively unrestricted growth, there is a mechanism change or other shift in the crystal growth process. Anisotropic crystal growth on different planes is likely to be the predominant factor in this case. It has been demonstrated (see, for example, Fig. 24 of reference[29]) that crystals of Ti_3SiC_2 are always anisotropic, forming sheet or disk shaped grains, the orientation of which corresponds to the basal planes of the hexagonal crystal structure of Ti_3SiC_2, i.e. the Ti_3SiC_2 crystals grows preferentially in the a–b plane and far slower along the c-axis. During the early stages of growth, the Ti_3SiC_2 crystals are surrounded by a matrix of intermediate phases TiC_x and $Ti_5Si_3C_x$ which are gradually separated by the new phase into isolated regions. However, as the Ti_3SiC_2 crystals grow larger they intersect each other and cease growing laterally. In the latter stages of the reaction (i.e. $f > 0.5$), they will have formed a three-dimensional framework, leaving only basal plane faces available for additional growth. The remaining intermediate phases then continue to react and deposit layers on the basal planes of the pre-existing Ti_3SiC_2 by a much slower one-dimensional crystal growth mechanism.

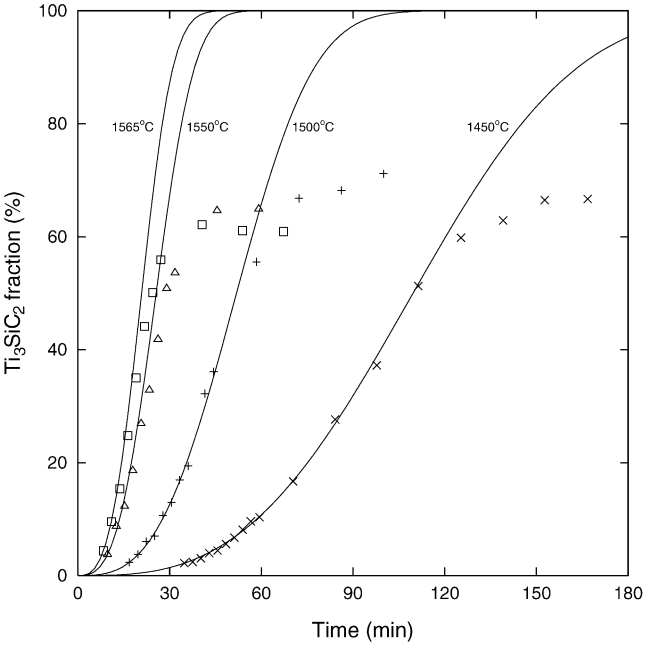

Fig. 3. The fraction of Ti_3SiC_2 vs. the total reaction time at various temperatures. The line at each temperature is fitted according to the MAJ equation. The symbols are the same as in Fig. 2.

Incompleteness of reaction between intermediate phases was a common feature of early attempts at bulk Ti_3SiC_2 synthesis and was also the case in these experiments (Fig. 3). The growth sequence outlined above may give some insight into the cessation (or extreme slowing) of the reaction. If some of the remaining intermediate phases are completely segregated (i.e. TiC_x or $Ti_5Si_3C_x$ only) due to isolation of the regions by the growing Ti_3SiC_2 crystals, they would be unable to react except by long-range diffusion of C and/or Si through the Ti_3SiC_2 crystals. Another contributing factor to incomplete reaction may have been evaporative loss of Si due to the use of a vacuum furnace.

In our previous in situ neutron diffraction study of the sintering of 3Ti/SiC/C mixtures using constant wavelength (CW) neutrons[16] a weak diffraction peak from Ti_3SiC_2 was detected between 2 and 4 h of heating at 1200 °C. However, in the current TOF experiment no Ti_3SiC_2 peak was found in

the diffraction patterns for 3Ti/SiC/C samples held at temperatures between 1200 and 1320 °C for 2 h and 10 min. Based on the kinetic information derived from the current measurements, the reaction rate K for the formation of Ti_3SiC_2 at 1200 °C would be $\sim 1.5 \times 10^{-6}\,s^{-1}$, which is about an order of magnitude lower than the estimate ($K(1200\,^{\circ}C) = (k \sim 2 \times 10^{-8})^{1/n} = 1.5 \times 10^{-5}\,s^{-1}$) made from the analysis of a single diffraction peak in our previous CW neutron diffraction data.[16] However, in our CW measurement at 1200 °C for a prolonged holding time the Avrami exponent derived for the reaction is ~1.6, and those earlier data should be treated with caution as only one weak peak from two diffraction patterns were used to construct the figures. The possible involvement of other competing reactions, e.g. $Ti + SiC \rightarrow Ti_5Si_3C + TiC_x$ at this lower temperature, and the difference of the sample environment (Ar gas for previous measurement, and vacuum in the TOF measurement) may have also played a role in the different behaviours of the samples at the same temperatures. This requires further investigation.

The value obtained for the reaction enthalpy (380 kJ/mol) is insensitive to the corrections made to the time scale and the upper temperature and so we have some confidence in it.

4. Conclusion

The kinetics of the growth of Ti_3SiC_2 crystals by solid state reaction of the intermediate phases TiC_x, $Ti_5Si_3C_x$ ($x \leq 1$) and a small amount of free C, determined from quantitative analysis of in situ neutron diffraction data collected at different temperatures may be modelled by the by Mehl–Avrami–Johnson equation.

Based on fitting the data with the Avrami equation, the value for the activation energy is 380 ± 10 kJ/mol, and the corresponding Avrami exponent is 3.0 ± 0.2 for the initial stages of crystal growth. The Avrami exponent decreases to approximately 1 after more than 0.5–0.6 of the reaction has completed. This phenomenon suggests a change in the mechanism of Ti_3SiC_2 crystal growth from three-dimensional to one-dimensional and indicates the importance of anisotropic crystal growth in the development of Ti_3SiC_2 microstructures.

Acknowledgments

The authors are grateful for the support of ISIS technical staff, particularly Chris Goodway. Funding support from the Australian Research Council—Discovery Grants and Linkage Infrastructure Equipment and Facilities Schemes, the Australian Institute of Nuclear Science and Engineering and the Access to Major Research Facilities Program is gratefully acknowledged.

References

1. Barsoum, M. W. and El-Raghy, T., Synthesis and characterization of a remarkable ceramic: Ti_3SiC_2. *J. Am. Ceram. Soc.*, 1996, **79**, 1953–1956.
2. Medvedeva, N., Novikova, D., Ivanovsky, A., Kuznetsov, M. and Freeman, A., Electronic properties of Ti_3SiC_2-based solid solutions. *Phys. Rev. B*, 1998, **58**, 16042–16050.
3. Myhra, S., Summer, J. W. B. and Kisi, E. H., Ti_3SiC_2—a layered ceramic exhibiting ultra-low friction. *Mater. Lett.*, 1999, **39**, 6–11.
4. Radhahrishnan, R., Williams, J. J. and Akinc, M., Synthesis and stability of Ti_3SiC_2. *J. Alloy. Comp.*, 1999, **285**, 85.
5. Yoo, H.-I., Barsoum, M. W. and El-Raghy, T., Ti_3SiC_2 has negligible thermopower. *Nature*, 2000, **407**, 581.
6. Du, Y., Schuster, J. C., Seifert, H. and Aldinger, F., Experimental investigation and thermodynamic calculation of the titanium–silicon–carbon system. *J. Am. Ceram. Soc.*, 2000, **83**, 197–203.
7. Riley, D. P., Kisi, E. H., Hansen, T. C. and Hewat, A. W., Self-propagating high-temperature synthesis of Ti_3SiC_2: I: ultra-high-speed neutron diffraction study of the reaction mechanism. *J. Am. Ceram. Soc.*, 2002, **85**, 2417–2424.
8. Wang, J. Y. and Zhou, Y. C., Ab initio investigation on the electronic structure and bonding properties in layered ternary compound Ti_3SiC_2 at high pressure. *J. Phys. Condens. Matter*, 2003, **15**, 1983–1991.
9. Goto, T. and Hirai, T., Chemically vapor deposited Ti_3SiC_2. *Mater. Res. Bull.*, 1987, **22**, 1195.
10. Pampuch, R., Lis, J., Stobierski, L. and Tymkiewicz, M., Ti_3SiC_2-based materials produced by self-propagating high-temperature synthesis (SHS) and ceramic processing. *J. Eur. Ceram. Soc.*, 1989, **5**, 283.
11. Barsoum, M. W. and El-Raghy, T., A progress report on Ti_3SiC_2, Ti_3GeC_2 and the H-phases, M_2BX. *J. Mater. Synth. Process.*, 1997, **5**, 197–216.
12. Goesmann, F., Wenzel, R. and Schmid-Fetzer, R., Preparation of Ti_3SiC_2 by electron-beam- ignitied solid-state reaction. *J. Am. Ceram. Soc.*, 1998, **81**, 3025–3028.
13. Zhou, Y. C., Sun, Z. M. and Yu, B. H., Microstructure of Ti_3SiC_2 prepared by the in situ hot pressing/solid-liquid reaction process. *Z. Metallkd.*, 2000, **91**, 937–941.
14. Riley, D. P., Kisi, E. H., Wu, E. and McCallum, A., Self-propagating high-temperature synthesis of Ti_3SiC_2 from $3Ti + SiC + C$ Reactants. *J. Mater. Sci. Lett.*, 2003, **22**, 1101–1104.
15. Zhang, Z. F., Sun, Z. M., Hashimoto, H. and Abe, T., Application of pulse discharge sintering (PDS) technique to rapid synthesis of Ti_3SiC_2 from Ti/Si/C powders. *J. Eur. Ceram. Soc.*, 2002, **22**, 2957–2961.
16. Wu, E., Kisi, E. H., Kennedy, S. J. and Studer, A. J., In situ neutron powder diffraction study of Ti_3SiC_2 synthesis. *J. Am. Ceram. Soc.*, 2001, **84**, 2281–2288.
17. Wu, E., Kisi, E. H., Riley, D. P. and Smith, R. I., Intermediate phases in Ti_3SiC_2 synthesis from Ti/SiC mixtures studied by time-resolved neutron diffraction. *J. Am. Ceram. Soc.*, 2002, **85**, 3084–3086.
18. El-Raghy, T. and Barsoum, M. W., Processing and mechanical properties of Ti_3SiC_2: I: reaction path and microstructure evolution. *J. Am. Ceram. Soc.*, 1999, **82**, 2849.
19. Smith, R. I., Hull, S. and Armstrong, A. R., The polaris powder diffractometer at ISIS. In *Proceedings of the 3rd European Powder Diffraction Conference, Vienna, Austria*, 1993, ed. R. Delhez and E. J. Mittemeijer. Material Science Forum, 1994, pp. 166–169, 251–256.
20. Larson, A. C. and Von Dreele, R. B., *Los Alamos National Scattering Center (LANSCE) Report No. MS-H805*. Los Alamos National Laboratory, Los Alamos, NM, 2000, http://lib-www.lanl.gov/la-pubs/00285897.pdf.

21. Hill, R. J. and Howard, C. J., Quantitative phase analysis from neutron powder diffraction data using the Rietveld method. *J. Appl. Cryst.*, 1987, **20**, 467.
22. Johnson, W. A. and Mehl, K. F., Reaction kinetics in processes of nucleation and growth. *Trans. Am. Inst. Min. Metall. Eng.*, 1932, **135**, 416–442.
23. Avrami, M., Kinetics of phase change: I: general theory. *J. Chem. Phys.*, 1939, **7**, 1103–1112.
24. Avrami, M., Kinetics of phase change: II: transformation–time relations for random distribution of nuclei. *J. Chem. Phys.*, 1940, **8**, 212–224.
25. Avrami, M., Kinetics of phase change: III: granulation, phase change, and microstructure. *J. Chem. Phys.*, 1941, **9**, 177–184.
26. Malek, J. and Mitsuhashi, T., Testing method for the Johnson–Mehl–Avrami equation in kinetic analysis of crystallization processes. *J. Am. Ceram. Soc.*, 2000, **83**, 2103–2105.
27. Sestak, J., Non-isothermal kinetics. *Proc. 3rd Intl. Conf. Therm. Anal. Davos*, 1971, **2**, 3–30.
28. Henderson, D. W., Experimental analysis of non-isothermal transformations involving nucleation and growth. *J. Thermal. Anal.*, 1979, **15**, 325–331.
29. Barsoum, M. W., The $M_{N+1}AX_N$ phases: a new class of solids: thermodynamically stable nanolaminates. *Prog. Solid State Chem.*, 2000, **28**, 201–281.